frontiers | Frontiers in Energy Research

TYPE Original Research
PUBLISHED 05 January 2024
DOI 10.3389/fenrg.2023.1334565

OPEN ACCESS

EDITED BY
Minglei Bao,
Zhejiang University, China

REVIEWED BY
Yizhou Zhou,
Hohai University, China
Tao Wu,
Southern Methodist University,
United States
Heping Jia,
North China Electric Power University,
China

*CORRESPONDENCE
Mingshun Liu,
lms2800@qq.com

RECEIVED 07 November 2023
ACCEPTED 11 December 2023
PUBLISHED 05 January 2024

CITATION
Liu M, Zhao Y, Zhu L, Chen Q and Chang D (2024), Co-evaluation of power system frequency performance and operational reliability considering the frequency regulation capability of wind power.
Front. Energy Res. 11:1334565.
doi: 10.3389/fenrg.2023.1334565

Co-evaluation of power system frequency performance and operational reliability considering the frequency regulation capability of wind power

Mingshun Liu[1]*, Yusheng Zhao[2], Lingzi Zhu[1], Qihui Chen[2] and Dongxu Chang[3]

[1]Power Dispatching and Control Center of Guizhou Power Grid Company, Guiyang, China, [2]State Key Laboratory of Power Transmission Equipment Technology, School of Electrical Engineering, Chongqing University, Chongqing, China, [3]CSG Key Laboratory for Power System Simulation, Electric Power Research Institute, China Southern Power Grid, Guangzhou, China

With the increasing proportion of renewable energy, the power system inertia decreases, and the operation uncertainty rises. It brings concerns about the system frequency and operational reliability. However, the impacts of the power system frequency performance on the reliability parameters of generation units have not been fully investigated. This paper studies the frequency performance and the operational reliability co-evaluation for power systems considering wind turbines. Firstly, a power system frequency regulation model is established considering the regulation capability of wind turbines. Then, the cluster of equivalent wind turbines is incorporated into the frequency regulation architecture of thermal power units, which accelerates the analysis of frequency performance. Then, the frequency performance of the power system with the participation of wind turbines under the operation uncertainty and the unit random faults is quantitatively analyzed. A frequency-dependent generator reliability parameter model is derived. Next, a multi-time scale co-evaluation framework is proposed to realize the co-evaluation of frequency performance and operational reliability. Case studies are carried out on the modified IEEE RTS-79 system and a provincial power system. Results show that compared with the existing research, the proposed method can obtain the frequency performance and reliability results efficiently.

KEYWORDS

renewable energy, wind turbines, power system reliability, frequency regulation, risk evaluation

1 Introduction

In line with China's "Carbon Peak and Carbon Neutrality" policy, the installed capacity of renewable energy units is expected to experience further growth. As stated in the National Development and Reform Commission's report 'China's Renewable Energy Development in 2022"(National development and reform commission of China, 2022), China's renewable energy installed capacity is projected to reach 1.2 billion kilowatts by 2022, accounting for 47.3% of the country's total power generation. This will result in a total renewable energy power generation of 2.7 trillion kW hours, representing 31.6% of the total electricity consumption in society. The State Grid Energy Institute has reported that China's wind and solar installed capacity is forecasted to reach 5 billion kilowatts by 2060, constituting over 65% of the total installed capacity (Lin et al., 2022a). Wind power, being the most mature and cost-effective renewable energy technology currently, is anticipated to witness a five-fold increase in installed capacity by 2060. Consequently, renewable energy will become the primary source of electricity supply in China.

The increasing integration of renewable energy sources, coupled with the retirement of conventional synchronous units like thermal power plants, has led to heightened uncertainty in the power supply of the electrical grid. Consequently, the system's inertia has decreased, posing challenges to the frequency security and operational reliability of the power system (Lin et al., 2023). One potential solution to address this issue is to involve wind power generators in economic dispatch and frequency regulation services (Zhang et al., 2022; Lei et al., 2022; Tang et al., 2022). In line with China's "Guidelines for Power System Safety and Stability" implemented on 1 July 2020, wind power generators are required to possess primary frequency regulation capabilities, with a higher priority assigned to primary frequency regulation than automatic power generation control (National Power Grid Operation And Control Standardization Technical Committee, 2023). It is foreseeable that wind power generators, as an increasingly significant energy source in modern power systems, will assume more substantial responsibilities in peak load management and frequency regulation.

The expansion of wind power generators integrated into the power grid leads to system frequency fluctuations, thereby influencing unit operation and dispatch as well as potentially impacting unit outage probabilities (Wu et al., 2023). Consequently, the operational and maintenance costs of the power system are likely to increase (Yang et al., 2020). Notably, augmented frequency fluctuations can trigger protective actions, such as frequency protection measures or even generator tripping, which are considered reliability events (Zhou et al., 2021). To illustrate this point, the British blackout incident in August 2019 serves as an example. The rapid decline in system frequency, resulting from transmission line and wind turbine failures, prompted the activation of frequency protection mechanisms in distributed generators, leading to their shutdown. This further exacerbated the frequency drop, ultimately necessitating the activation of the system's low-frequency load-shedding mechanism. Consequently, approximately 931 MW of load was disconnected, resulting in the shutdown of local industries and commerce, paralyzing transportation, and incurring significant economic losses (Owens, 2019). These events demonstrate the interconnected nature of system frequency performance and operational reliability. Therefore, it becomes imperative to conduct a comprehensive assessment of the power system's operational reliability level and frequency performance.

Various studies have investigated methods for assessing the operational reliability of power systems considering the uncertainty of wind power. These methods include analytical approaches (Sharifinia et al., 2020), time-series Markov Monte Carlo methods (Chao et al., 2019), and Monte Carlo hybrid sampling methods (Ding, 2022; Li, 2013; Wu and Wang, 2023) is a pioneering work in the reliability evaluation for integrated electricity-gas systems considering hydrogen. (Ding et al., 2021). provides a comprehensive study for the operational reliability assessment of the integrated heat and electricity system. (Hu et al., 2021). focuses on the power system operational reliability assessment considering the decision-dependent uncertainty. These studies propose an efficient reliability evaluation method for power systems. However, they overlook the impact of frequency performance on system reliability and fail to comprehensively capture the interplay between frequency performance and reliability parameters. The uncertainty in wind power output directly leads to increased system frequency fluctuations. Then the protection device of the generation units may be triggered and even result in generator trips, which are considered reliability events. These events ultimately affect the outage probability of generating units and consequently impact the results of power system operational reliability assessments (Kundur and Malik, 2022).

Currently, there are a limited number of studies that address the comprehensive assessment of power system frequency performance and operational reliability. A collaborative frequency regulation architecture combining battery energy storage and generators is proposed in (Farivar et al., 2022) to achieve a comprehensive evaluation of frequency performance and operational reliability. (Ye et al., 2023). presents a comprehensive evaluation method considering the frequency performance reliability of interconnected power systems, considering the characteristics of high-voltage DC transmission. These studies primarily analyze the impact of frequency regulation on the output power of generators, overlooking the influence of system frequency performance on the reliability parameters of the generation units. Moreover, they fail to adequately consider the frequency regulation capabilities of wind turbine clusters and neglect factors such as the wake effect of wind turbine clusters, leading to overly optimistic reliability assessment results (Wang et al., 2020).

This study aims to address the coupling effect between power system frequency performance and generator unit reliability parameters. Contributions of this paper are.

1) Propose an analytical expression of the frequency-dependent reliability parameters for generation units. The frequency performance of the power system is quantitatively analyzed under load uncertainty and random unit failures.
2) Formulate a comprehensive assessment method that incorporates the frequency regulation capability of wind turbine clusters, which enables the comprehensive evaluation of secondary frequency dynamics and hour-level power system operational reliability.
3) Numerical examples are conducted using the modified IEEE RTS-79 system and a provincial power system to validate the accuracy of the proposed method. The results obtained from this research contribute to the verification of the method's effectiveness and provide valuable insights for secondary frequency control and reliability optimization efforts.

The rest of this manuscript is organized as follows. Section 1 introduces the frequency regulation model of wind turbine clusters. Section 2 proposes the frequency-dependent reliability parameters of generation units and the power system operational reliability assessment model. Section 3 formulates the power system frequency-reliability comprehensive assessment framework. Case studies are illustrated in Section 4. Section 5 concludes this paper.

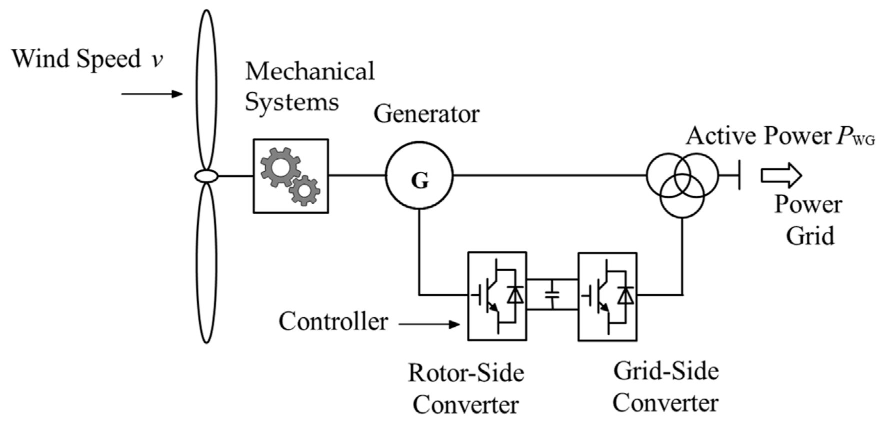

FIGURE 1
The structure of the wind turbine.

2 Frequency regulation model of wind turbine clusters

2.1 Frequency regulation model of doubly-fed induction wind turbine

Doubly-fed induction generator converters (DFIG) wind turbines consist of several essential components, including wind turbines, mechanical systems, generators, converters, controllers, and associated devices, as shown in Figure 1. The primary function of the wind turbine component is to extract energy from the wind and convert it into mechanical energy. This mechanical energy is subsequently transmitted through the mechanical system, enabling the rotation of the generator. The generator, an induction machine in this case, converts the mechanical energy into electrical energy. To achieve variable speed constant frequency power generation, a converter is interconnected with the rotor of the generator. The converter plays a crucial role in regulating the excitation current frequency of the rotor, thereby maintaining a constant stator frequency. Through this control mechanism, the DFIG can operate at varying speeds while ensuring a consistent frequency of the generated electrical power.

To provide frequency regulation services, DFIG works in sub-optimal power point tracking mode. In this mode, the DFIG reserves a certain amount of wind power and collects the frequency deviation of the power system Δf and frequency change rate df/dt to adjust its output. The wind turbine output power P_{WG} can be established as a piece-wise nonlinear function of the wind turbine rotor speed w_G (Lin et al., 2022b):

$$P_{\mathrm{WG}} = \begin{cases} \dfrac{Kw_0^3\left(w_{\mathrm{G}} - w_{\mathrm{min}}\right)}{\left(w_0 - w_{\mathrm{min}}\right)}, & w_{\mathrm{min}} < w_{\mathrm{G}} < w_0 \\ Kw_{\mathrm{G}}^3, & w_0 \le w_{\mathrm{G}} \le w_1 \\ \dfrac{\left(P_{\mathrm{m}} - Kw_1^3\right)\left(w_{\mathrm{G}} - w_{\mathrm{max}}\right)}{\left(w_{\mathrm{max}} - w_1\right)} + P_{\mathrm{m}}, & w_1 < w_{\mathrm{G}} < w_{\mathrm{max}} \\ P_{\mathrm{m}}, & w_{\mathrm{G}} \ge w_{\mathrm{max}} \end{cases} \tag{1}$$

where w_{min} represents the starting speed of the fan rotor; w_0 represents the rotor speed in the constant speed zone of the fan; w_{max} represents the speed at which the DFIG enters the constant power zone; P_{m} represents the maximum output power of the DFIG; K is the power tracking coefficient. The value of the power tracking coefficient K depends on the power system frequency deviation Δf and frequency change rate $\mathrm{d}f/\mathrm{d}t$ such that

$$K = K_{\mathrm{max}}\left(u_{\mathrm{OPPT}} - \Delta u_{\mathrm{OPPT}}\right) \tag{2}$$

where K_{max} is the power tracking coefficient of the DFIG operating in the maximum power tracking mode; u_{OPPT} is the virtual inertia factor of the DFIG; Δu_{OPPT} is the correction coefficient of the virtual inertia factor of the DFIG. The relationship between the virtual inertia factor u_{OPPT} and power system frequency deviation Δf is

$$u_{\mathrm{OOPT}} = w_{\mathrm{G0}}^3\left(w_{\mathrm{G0}} + \frac{2\pi c\Delta f}{p}\right)^{-1} \tag{3}$$

where w_{G0} is the rotor speed when the wind turbine participates in frequency regulation; c is the virtual inertia coefficient of the wind turbine; p is the number of pole pairs of the wind turbine.

The relationship between the wind turbine virtual inertia factor correction coefficient and the power system frequency change rate is (Shafi et al., 2020)

$$\Delta u_{\mathrm{OPPT}} = \frac{2w_{\mathrm{G0}}w_{\mathrm{s}}^{-1}cHf}{K_{\mathrm{max}}w_{\mathrm{G}}^3} \cdot \frac{w_{\mathrm{G}}^2 - w_{\mathrm{min}}^2}{w_{\mathrm{max}}^2 - w_{\mathrm{min}}^2} \cdot \frac{\mathrm{d}f}{dt} \tag{4}$$

where w_{s} is the grid synchronous rotor speed; H is the equivalent inertia time constant of the DFIG.

$$\Delta P_{WT} = 2\left(\frac{w_{\mathrm{G0}}}{w_s}cH\right)f\frac{df}{dt} \tag{5}$$

Figure 2 shows the relationship between the output power of the wind turbine, the rotor speed, and the wind speed based on Eqs 1–5. It is assumed that before the disturbance occurs, the wind turbine operates at point A. When the system frequency decreases, the frequency changes, i.e., $\Delta f < 0$. According to Equation 3 and Equation 2, the virtual inertia factor of the wind turbine u_{OOPT} decreases. Then the power tracking coefficient K increases and the wind turbine operating curve changes from the purple curve in Figure 2 to the red curve. The operating point moves from point A to

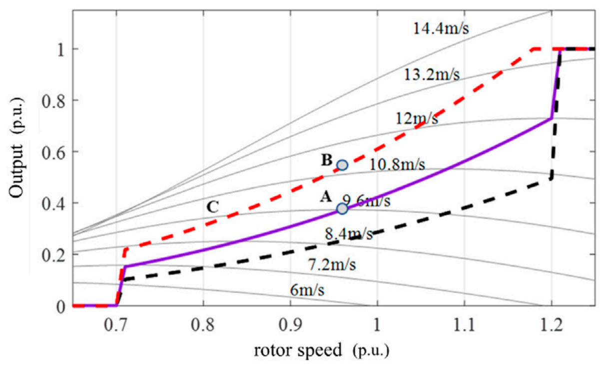

FIGURE 2
The relationship among the output power of the wind turbine, the rotor speed, and the wind speed.

B point, thereby increasing the output power of the wind turbine P_{WG}. Under this circumstance, the input mechanical power of the wind turbine remains at the level of point A. Therefore, the wind turbine will only work at point B for a short time. Then slowly fall back to point C where the input mechanical power and output electromagnetic power are balanced. Point C is not the optimal operating point at this wind speed. In consideration of the operating economy, the output power of the wind turbine will be adjusted back to operating point A. The moving trajectories of the wind turbine's working points are A, B, C, and A in sequence. Figure 3 shows the frequency regulation model of a single wind turbine.

2.2 Frequency regulation model of wind turbine cluster considering wake effects

Since the frequency regulation capability of a single wind turbine is weak, clusters of wind turbines often participate in power system frequency regulation. In wind turbine clusters, the wake effect refers to the phenomenon that upstream wind turbines absorb part of the wind energy, thereby affecting the wind speed of downstream wind turbines. Ignoring this phenomenon will lead to overly optimistic evaluation results of power system frequency performance and reliability. This paper uses the common Jensen model to characterize the wake effect in wind turbine clusters (Zhao et al., 2021), as shown in Figure 4.

In Figure 4, v_i is the wind speed of the upstream fan; v_j is the wind speed of the down-stream fan; r_i is the blade radius of the upstream fan; α is the wake drop coefficient; R_i represents the influence range of the wake, satisfying $R_i = r_i + \alpha\ x_{ij}$; x_{ij} represents the up-stream wind turbine unit i and the downstream. The distance between wind turbines j along the wind direction. Part of the wind energy of the downstream wind turbine j is blocked by the upstream wind turbine i, and the blocked area is recorded as S_{ij}. S_j is the wind-catching area of wind turbine j. The downstream affected area increases as the attenuation coefficient α increases. The wind speed reaching the downstream wind turbine j is not only affected by the upstream wind turbine i directly in front of it, but also by other upstream wind turbines.

Based on the Jensen model, the wind speed v_j of the downstream wind turbine can be estimated as

$$v_j = \beta_j v_i \tag{6}$$

$$\beta_j = 1 - \sum_{i=1}^{n} \left(1 - \sqrt{1 - C_i}\right) \frac{r_i^2 S_{ij}}{R_i^2 S_j} \tag{7}$$

where C_i is the thrust coefficient of the upstream fan i, which is related to the operating status of the fan i itself; n is the total number of upstream fans of the fan j. β_j is the wake effect coefficient of wind turbine j, which comprehensively reflects the influence of the wake effect. The smaller β_j is, the greater the wake effect will be, and the weaker the frequency modulation ability of the downstream fan will be.

When a wind turbine cluster contains hundreds or even thousands of wind turbines, it is impossible to analyze the frequency regulation capabilities of the units under the influence of the wake effect and its impact on system reliability. Therefore, this paper proposes a clustering method based on the wake effect coefficient to classify wind turbine clusters according to the wake effect coefficient of each wind turbine. The classification number is $A, B, C, \cdots$, and the corresponding wind turbine set is recorded as $\Omega_A, \Omega_B, \cdots$. Wind turbines of the same type do not affect each other, but the output of wind turbines of different types is affected by the wind turbines of the previous type. If wind turbines of the same type

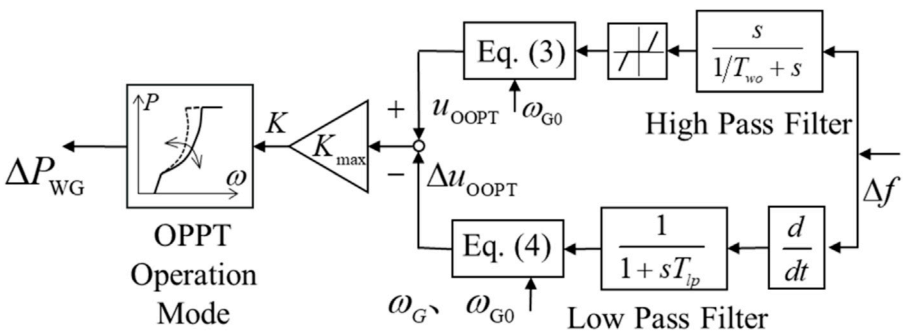

FIGURE 3
Frequency regulation model of a single wind turbine.

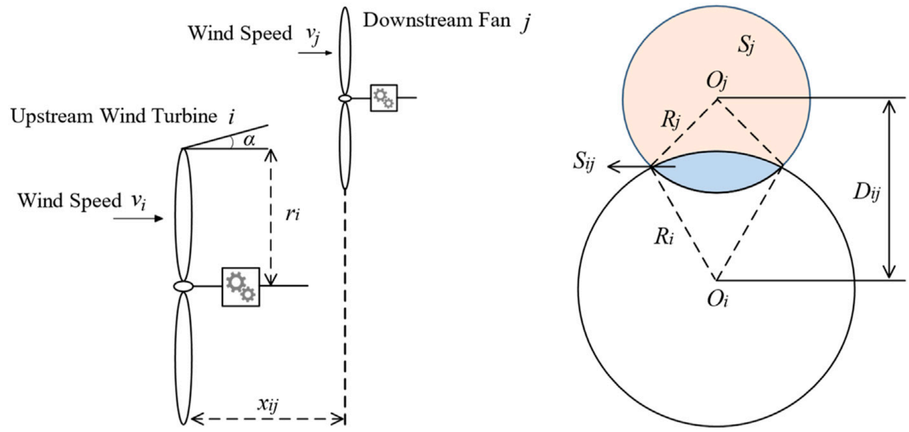

FIGURE 4
Schematic diagram of wake effect of wind turbine cluster based on Jensen model.

are subjected to the same wind speed, the thrust coefficients of the turbines C_i are the same.

Since the influence coefficient of the wake effect is nonlinearly related to factors such as the spatial position of the wind turbine, blade size, relative distance, *etc.*, it presents characteristics of randomness and convexity that are difficult to guarantee. Therefore, this paper uses a density-based clustering algorithm with the wake effect coefficient as the core index to solve the problem of overestimation of wind turbine frequency regulation capabilities and power system operational reliability assessment caused by inaccurate clustering of wind turbines and inaccurate wind speed estimation. The problem with being too optimistic.

After the clustering is completed, the withstand wind speed of each type of wind turbine can be calculated. For example, the wind speed of Class B wind turbines is affected by the wake effect caused by Class A wind turbines. The wind speed is recorded as $v_{j,B}$, which can be expressed as

$$v_{j,\mathrm{B}} = \beta_{j,\mathrm{B}} v_{\mathrm{A}} \tag{8}$$

$$\beta_{j,\mathrm{B}} = 1 - \sum_{i\in\Omega_A}\left[\left(1-\sqrt{1-C_{\mathrm{A}}}\right)\frac{r_i^2 S_{ij}}{R_i^2 S_j}\right] \tag{9}$$

where v_{A} is the wind speed of class A wind turbine; C_{A} is the thrust coefficient of class A wind turbine; $\beta_{j,\mathrm{B}}$ is the wake effect influence coefficient of wind turbine j belonging to class B under the influence of the wake effect of class A wind turbine. The wind turbine cluster frequency regulation model considering the wake effect is shown in Figure 5 based on Eqs 6–9.

3 Power system operational reliability assessment model

3.1 Power system frequency regulation model

By incorporating the wind turbine cluster frequency regulation model, a wind turbine cluster-thermal power collaborative frequency regulation model is obtained, as shown in Figure 6.

The collaborative frequency regulation model between wind turbine clusters and thermal power units, as depicted in Figure 6, incorporates various factors such as the reserve capacity, ramping power limit of the thermal power unit, and the frequency regulation module of the wind turbine cluster. This model facilitates the transition from isolated analysis to integrated evaluation of these two distinct resource types, thereby extending the assessment framework. Each symbol in Figure 6 is explained as follows: R is the equivalent coefficient of the governor of the reheated thermal power generation unit; T_{CG} is the equivalent time constant of the governor; T_{CH} is the equivalent time constant of the steam chamber; F_{HP} is the high-pressure power of the steam turbine. T_{RH} is the steam turbine equivalent time constant. ΔP_{CG} is the thermal power unit output change. M_{CG} is the system load-damping coefficient. T_{CG} is the system inertia equivalent constant. A is the system frequency deviation factor, satisfying $A = D + 1/R$. System power deficit ΔP_{D} caused by wind power output fluctuations ΔP_{DW} , unit failures ΔP_{DC} , and load fluctuations ΔP_{DL}; that is, $\Delta P_{\mathrm{D}} = \Delta P_{\mathrm{DW}} + \Delta P_{\mathrm{DC}} + \Delta P_{DL}$.

Note that the set of thermal power units participating in secondary frequency regulation is Ω_{CG}. The set of thermal power units with occasional failures is $\Omega_{\mathrm{CG}}^{\mathrm{fault}}$. The set of thermal power units operating normally is $\Omega_{\mathrm{CG}}^{\mathrm{normal}}$. The output variation of the thermal power generating unit can be expressed as

$$\Delta P_{\mathrm{CG}} = \sum_{i\in\Omega_{\mathrm{CG}}^{\mathrm{normal}}} \Delta P_{\mathrm{CG},i} \tag{10}$$

where $\Delta P_{\mathrm{CG},i}$ is the output change amount of thermal power generating unit i. The wind turbine cluster-thermal power generation unit collaborative frequency regulation strategy is not the research scope of this article. Thus, this article directly adopts the frequency control strategy proposed in (Huang et al., 2023).

3.2 Frequency-dependent generator reliability parameter model

The reliability parameters of the generator (such as outage probability) are related to the health status of the generator, the

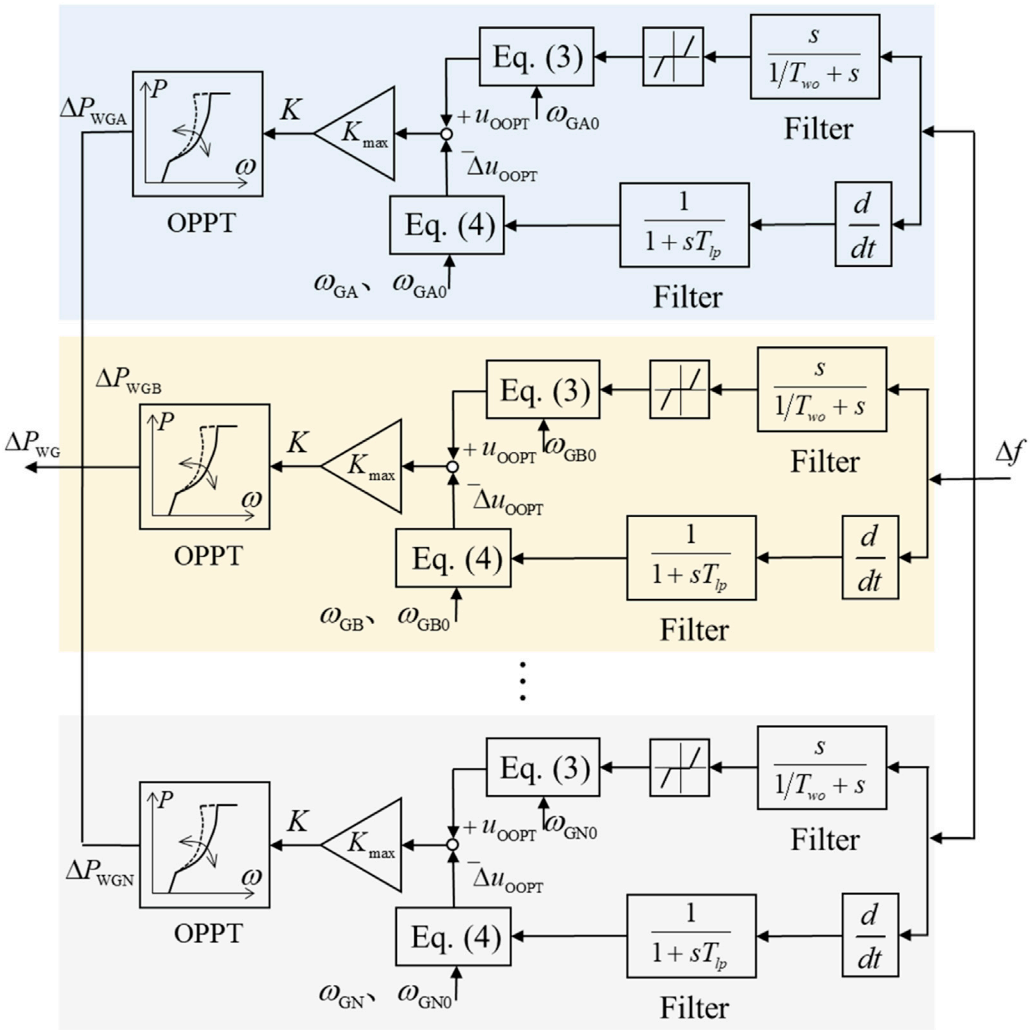

FIGURE 5
Frequency regulation model of wind turbine cluster considering the wake effect.

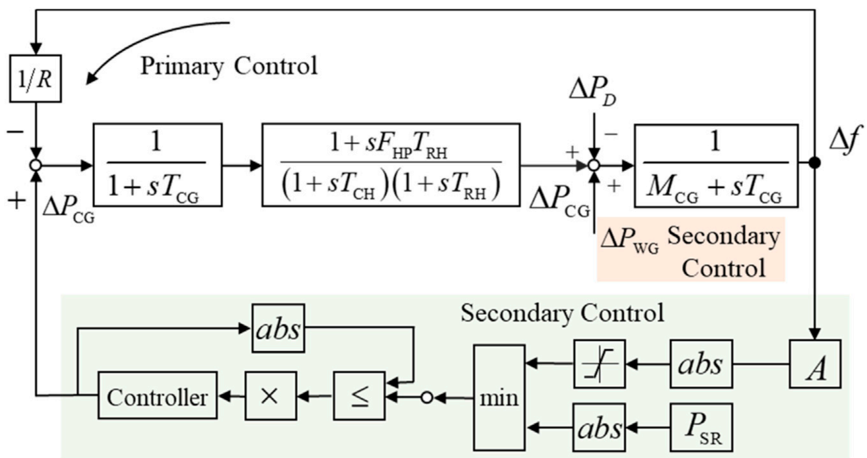

FIGURE 6
Wind turbine cluster-thermal power coordinated frequency regulation model.

external environment, and the system operating conditions. Specifically, the reasons for the outage of the generating set may be.

1) Actual failure of the generating set due to aging, extreme high temperature, or cold wave.
2) Abnormal operation of the system (such as frequency exceeding the limit) causes the protection device to operate and power generation The unit was not faulty but was removed from the power grid, causing an outage in a nonfaulty state.
3) Human misoperation and protection malfunction.

When establishing a generator reliability parameter model, this article focuses on the impact of reasons 1) and 2) on the generator reliability parameters due to the low probability of human misoperation and protection malfunction. The impact of reason 1) on the outage probability U of the generator is U_1, and the impact of reason 2) on the outage probability U of the generator is U_2. Since reasons 1) and 2) are independent events, the probability of generator outage satisfies

$$U = U_1 + U_2 - U_1 U_2 \tag{11}$$

The Weibull model is used to describe the influence of the aging degree of the generator on the probability of outage of the generator and the probability of outage due to aging Δt_G after the generator continues to operate for t_G years is obtained

$$U_1 = \frac{\int_{t_G}^{t_G+\Delta t_G} \frac{\beta \cdot t^{\beta-1}}{\alpha^{\beta}} e^{-\left(\frac{t}{\alpha}\right)^{\beta}} dt}{\int_{t_G}^{\infty} \frac{\beta \cdot t^{\beta-1}}{\alpha^{\beta}} e^{-\left(\frac{t}{\alpha}\right)^{\beta}} dt} \tag{12}$$

where t is the running time of the generator in years; α is the size parameter of the generator; β is the shape parameter of the generator. α and β jointly reflect the impact of the aging degree of the generator on the outage rate.

Analyze the impact of reason 2) on the outage rate of generating units. The generator is equipped with a complete and sensitive relay protection system to ensure that the generator operates within a reasonable frequency range. When the generator operates within the low-frequency/high-frequency protection threshold range of the generator, the frequency does not affect the probability of outage of the generator. The probability of an outage of the generator is linked to the aging degree of the generator. Currently, $U_2 = 0$ and $U = U_1$. When the generator reaches the protection threshold of the generator frequency protection device, the protection device starts, and the generator is cut off from the grid. Although the generator is not faulty currently, it does not help maintain the power balance. For the power grid, the generator is equivalent to being out of service currently. Under this circumstance, the generator outage probability is 1, $U = U_2 = 1$. In the context where the system frequency falls within the range of the normal value and the protection-action value, a direct correlation exists between the probability of generator failure and the frequency level, which can be expressed as Eq. 13

$$U(f) = \begin{cases} \dfrac{(U_1 - 1)f + f_{\mathrm{g,\,min}}^{\mathrm{normal}} - U_1 f_{\mathrm{g,\,min}}^{\mathrm{protect}}}{f_{\mathrm{g,\,min}}^{\mathrm{normal}} - f_{\mathrm{g,\,min}}^{\mathrm{protect}}} & f_{\mathrm{g,\,min}}^{\mathrm{protect}} \le f \le f_{\mathrm{g,\,min}}^{\mathrm{normal}} \\[2ex] \dfrac{(1 - U_1)f + U_1 f_{\mathrm{g,\,max}}^{\mathrm{protect}} - f_{\mathrm{g,\,max}}^{\mathrm{normal}}}{f_{\mathrm{g,\,max}}^{\mathrm{protect}} - f_{\mathrm{g,\,max}}^{\mathrm{normal}}} & f_{\mathrm{g,\,max}}^{\mathrm{normal}} \le f \le f_{\mathrm{g,\,max}}^{\mathrm{protect}} \end{cases} \tag{13}$$

where f protects g, min and f protect g, max is the generator's low- and high-frequency protection action values. The generator will trip when the frequency is f protect g, min or f protect g,max.

The two-state Markov model is used to describe the reliability parameter model of the generator. Based on calculating the probability of generator outage, the generator outage rate can be determined. Since the generator outage probability is related to the system frequency, without loss of generality, note $U = U(f)$. Then the generator outage rate can be written as

$$\lambda(f) = \frac{\mu \cdot U(f)}{1 - U(f)} \tag{14}$$

where μ is the repair rate of the generator (the unit is timed/year), which is given by historical statistical data. Based on the Markov limit state equation, it can be obtained that the steady-state probability of the generator unit in normal operation is $\mu/(\lambda(f) + \mu)$, and the steady-state probability of the generator in outage state is $\lambda(f)/(\lambda(f) + \mu)$.

3.3 Power system risk assessment indicators

This paper uses reliability indicators in terms of power and probability to quantify the ability of the power system to meet users' power frequency quality and power demand, including 1) expected energy not supplied (EENS), 2) expected indirect energy not supplied (EIENS), 3) expected number of under-frequency events (ENUF), 4) expected under frequency duration (EUFD), 5) probability of low-frequency events (LFEP) and 6) the probability of the system recovering from the low-frequency event (PRLFE). The detailed definitions of these metrics are referred to Eqs 14–21.

1) EENS represents the risk of load loss in the power system within a period and is the product of the probability of a load loss event and the amount of load loss. Let the expected power shortage be M_{EENS} , which can be expressed as

$$M_{\mathrm{EENS}} = \sum_{k \in S} p_k \cdot (\Delta P_{\mathrm{D}} - \Delta P_{\mathrm{CG}} - \Delta P_{\mathrm{WG}}) T_H \tag{15}$$

where the set of loss-of-load events is S; the loss-of-load event is k; the probability of occurrence of a loss-of-load event is p_k; $\Delta P_{\mathrm{D}} - \Delta P_{\mathrm{CG}} - \Delta P_{\mathrm{WG}}$ is the amount of load loss caused by source load fluctuations and sporadic failures of generator units in the power system; T_{H} is the duration of the loss-of-load even.

2) EIENS represents insufficient power during the primary and secondary frequency adjustment process. The power shortage here does not appear as load loss but as a frequency deviation of the power system. The indirect expected power shortage EIENS is defined as

$$M_{\mathrm{EIENS}} = \sum_{k \in S} p_k \cdot \left(M_{\mathrm{IENS},k,1} + M_{\mathrm{IENS},k,2}\right) \tag{16}$$

where $M_{\mathrm{IENS},k,1}$ and $M_{\mathrm{IENS},k,2}$ respectively represent the indirect power shortage reflected by the frequency deviation of the next and secondary frequency modulation processes of event k. It is recorded

10.3389/fenrg.2023.1334565

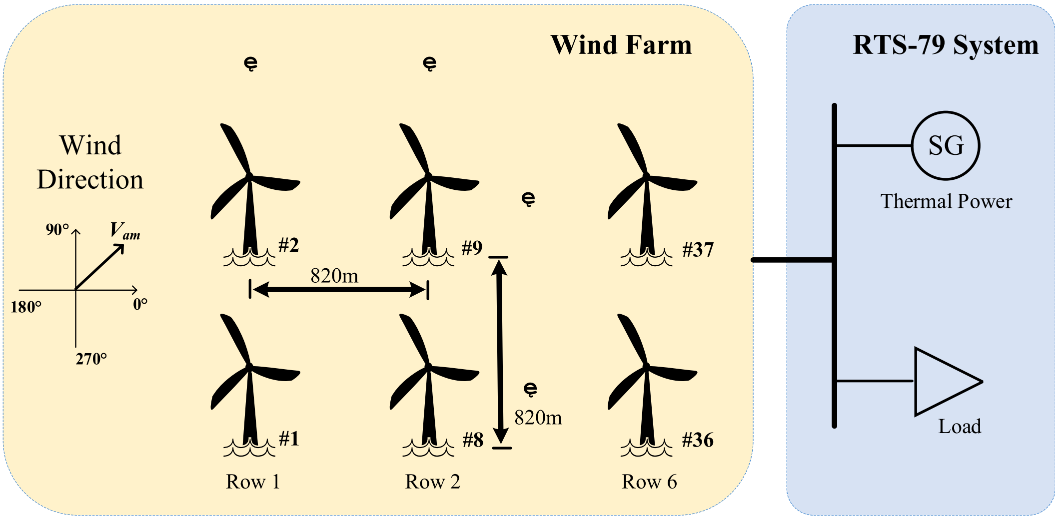

FIGURE 7
The modified IEEE RTS-79 system.

that the system frequency deviation at the end of the first frequency modulation is $\Delta f_{1,end}$, the duration of the first frequency modulation Δt_1, and the corresponding active power deficit is $\Delta P_{1,end}$. At the end of the second frequency modulation, the system frequency deviation is $\Delta f_{2,end}$; the duration of the second frequency modulation is Δt_2; and the corresponding active power deficit is $\Delta P_{2,end}$. Then the indirect power shortage in the next secondary frequency modulation process of event k $M_{\mathrm{IENS},k,1}$ and $M_{\mathrm{IENS},k,2}$ satisfies

$$M_{\mathrm{IENS},k,1} = \Delta P_{1,end}\Delta t_1 \tag{17}$$

$$M_{\mathrm{IENS},k,2} = \left(\Delta P_{1,end} - \frac{\Delta P_{2,end}}{2}\right)(\Delta t_2 - \Delta t_1) \tag{18}$$

3) ENUF represents the number of frequency limit violations within a period. The expectation of recording frequency exceeding the limit is M_{ENUF} , which is defined as

$$M_{\mathrm{ENUF}} = \sum_{k\in S} p_k \cdot N_{\mathrm{NUF},k} \tag{19}$$

where $N_{\mathrm{NUF},k}$ is the number of times the system frequency exceeds the limit under event k, satisfying $N_{\mathrm{NUF},k} \in \{0,1,2\}$. If the frequency limit does not occur in event k, then $N_{\mathrm{NUF},k} = 0$. If the frequency exceeds the limit and the frequency returns to a reasonable range after the frequency adjustment process, then $N_{\mathrm{NUF},k} = 2$; $N_{\mathrm{NUF},k} = 1$ otherwise.

4) EUFD characterizes the duration of low-frequency phenomena within a period. The expected duration of low frequency is recorded as M_{EUFD}, which is defined as

$$M_{\mathrm{EUFD}} = \sum_{k\in S} p_k \cdot T_{\mathrm{UFD},k} \tag{20}$$

where $T_{\mathrm{UFD},k}$ is the duration of the low-frequency phenomenon in event k.

5) LFEP is used to analyze the probability of low-frequency events in the system. The probability of occurrence of low-frequency events is recorded as M_{LFEP}, which can be defined as

$$M_{\mathrm{LFEP}} = \sum_{k\in S_{\mathrm{LFEP}}} p_k \tag{21}$$

where S_{LFEP} is the set of events that recover from low frequency to a reasonable frequency range.

4 Frequency-reliability comprehensive assessment framework

This section proposes a multi-time scale power system frequency performance-reliability comprehensive assessment process to couple the power system frequency adjustment process with the reliability assessment process. The evaluation process includes three links: power system event generation, event analysis, and indicator calculation.

This article employs the enumeration method to generate states for analysis. In comparison to sequential and non-sequential Monte Carlo methods, the enumeration method offers distinct advantages, such as clearer physical interpretations and more precise evaluation results.

In the state analysis process, the impact of the frequency regulation process needs to be considered. Take an event k as an example to illustrate. In event k, firstly, the power system generates power imbalance ΔP_D due to the source and load uncertainty and sporadic failures of equipment such as generating units. Subsequently, following the power imbalance, two distinct effects arise. Firstly, the power imbalance triggers frequency fluctuations within the power system, thereby influencing the reliability parameters of the generator and altering the event occurrence probability. Secondly, as per the established control strategy, the power system engages in one or

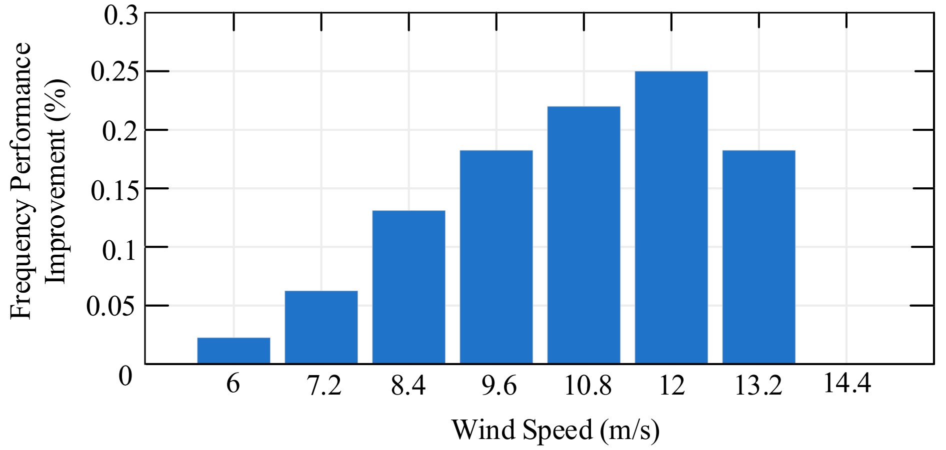

FIGURE 8
The improvement of the frequency performance with different wind speeds.

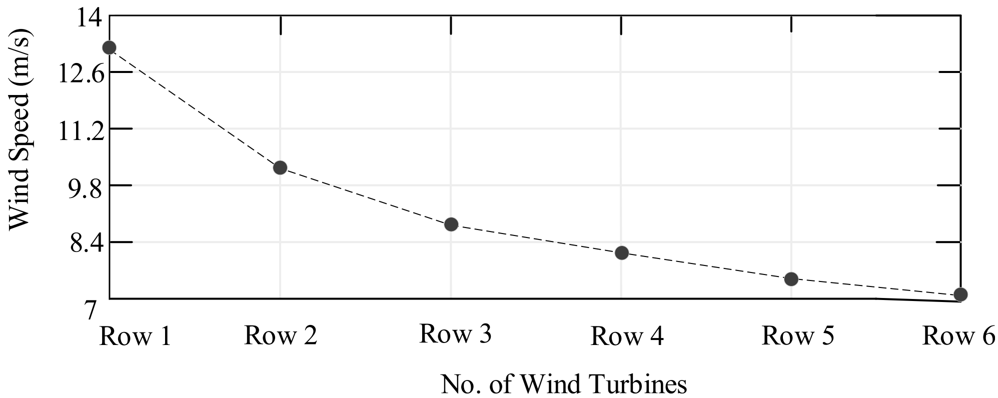

FIGURE 9
The wind speed of the wind turbine considering the wake effect.

TABLE 1 The parameters of the wind turbines.

Type	Inertia constant (MWs)	Ramping rate (MW/h)	Frequency regulation coefficient (MW/Hz)	Number
Wind Turbine	—	—	—	681
U12	2.5	60	4.8	3
U20	3.0	80	8.2	2
U50	4.0	300	25	2
U76	4.5	304	33	2
U100	5.5	300	57	2
U155	6.5	620	79	2
U197	7.5	591	109	2
U350	8.5	350	200	1
U400	10	1,000	267	2

TABLE 2 Cluster results of wind turbines under different wind directions.

Wind direction	Clustering results					
0°	Area 1	Area 2	Area 3	Area 4	Area 5	Area 6
	Group 1	Group 2	Group 3	Group 4	Group 5	Group 6
	1–7	8–14	15–21	22–28	29–35	36–42
18°	Area 1	Area 2		Area 3		
	Group 1	Group 2	Group 3	Group 4	Group 5	Group 6
	1–15, 22, 29, 36	16–21	23–28	30, 37	31–35	39–42
32°	Area 1	Area 2		Area 3		
	Group 1	Group 2	Group 3	Group 4	Group 5	Group 6
	1–15, 22, 29, 36	16–21, 23, 30, 37	24–28	31, 38	32–35	39–42
45°	Area 1	Area 2	Area 3	Area 4	Area 5	Area 6
	Group 1	Group 2	Group 3	Group 4	Group 5	Group 6
	1–8, 15, 22, 29, 36	9–14, 16, 23, 30, 37	17–21, 24, 31, 38	25–28, 32, 39	33–35, 40	41, 42

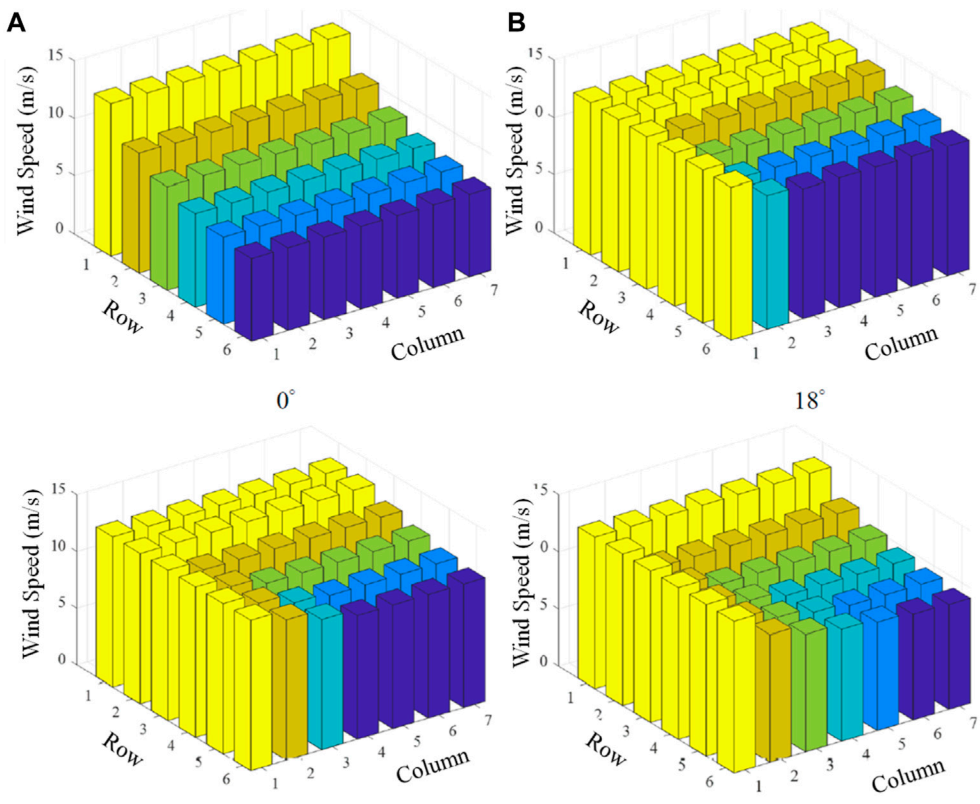

FIGURE 10
Cluster results of wind turbines under different wind directions. **(A)** The wind direction is 0°. **(B)** The wind direction is 18°. **(C)** The wind direction is 32°. **(D)** The wind direction is 45°.

two frequency regulations. This frequency regulation process, in turn, generates an indirectly expected power shortage. Consequently, the power imbalance after undergoing frequency regulation is represented by $\Delta P_D - \Delta P_{CG} - \Delta P_{WG}$. If the imbalance is not 0, the power system must reduce the load, which occurs in the reliability event.

In the reliability metrics calculation process, the metrics are calculated based on the indicator definition and event analysis results.

TABLE 3 The results of the frequency performance and the operational reliability.

Index	Situation 1	Situation 2
M_{EENS} (MWh/year)	259,327	254,577
M_{EIENS} (MWh/year)	87,937	85,559
M_{ENUF} (occ./year)	4,867.4	4,747.6
M_{EUFD} (h/year)	161.7	149.8
M_{PLFE}	1	1
M_{PRFEL}	0.9413	0.9297

The power system frequency performance-reliability comprehensive assessment process is as follows.

Step 1: Input wind speed, wind turbine spatial position, load, traditional unit operating status, frequency control model parameters, generator unit reliability parameters, and other related parameters. The parameters of wind turbines are listed in Table 1.

Step 2: Use the enumeration method to generate the power system event set *S*. Perform status analysis on the events in the set *S* in turn. The status analysis is described in steps 3–6.

Step 3: Consider the event $k \in S$. The wind turbine clusters are clustered by considering the operating status of the wind turbine cluster, wind speed, wind direction, wind turbine cluster, and other factors. According to Equations 5–8, calculate the equivalent parameters of each type of wind turbine, such as wind speed, fan thrust coefficient, *etc.*

Step 4: Based on the wind turbine cluster-thermal power collaborative frequency regulation model, calculate the frequency response curve of the power system.

Step 5: According to the frequency response curve of the power system, record the frequency deviation amount at the end of the first and second frequency modulation of the system, whether the low-frequency event occurs, and its duration.

Step 6: According to the power system frequency response curve and Equations 10–12, update the steady-state outage probability and normal operation probability of the generating unit. Update the occurrence probability p_k of event *k*. Calculate system frequency performance and reliability metrics.

Step 7: Check whether the entire system status has been analyzed. If not, let $= k + 1$, and repeat steps 3 to 6.

5 Case study

This paper uses the modified IEEE RTS79 system and a provincial power system to evaluate the power system frequency performance and operational reliability. It verifies the necessity of considering the impacts of the system frequency performance on the operational reliability level.

TABLE 4 The system reliability evaluation results under four scenarios.

Index situation	M_{EENS} (MWh/year)	M_{EIENS} (MWh/year)
Situation A	259,327	87,937
Situation B	256,713	86,715
Situation C	254,577	85,559
Situation D	482,630	—

5.1 IEEE RTS79 system settings

The IEEE RTS79 system contains 9 types of conventional units and 1 wind turbine cluster. Assuming that the working life of all units is within the range of 3–5 years, the outage probability of generation units caused by aging can be calculated by Equation 11. The ramping rate, inertia constant, and frequency modulation coefficient of the generation units are referenced from (Attabo Ameh et al., 2023). The rated power of a single wind turbine is 1.5 MW, and the wind turbine control parameters can be found in (Chen et al., 2017). The wind power penetration rate is selected to be 30%. The load is set to a peak load of 2,850 MW and a load adjustment coefficient of 75 MW/Hz. The normal frequency of the system is 50 Hz, and the reasonable operating range of frequency is [49.8, 50.2] Hz. Only fault events of order 4 and below are considered in the reliability assessment. The time scale of each scenario is 1 h. It is assumed that all thermal power units participate in the primary and secondary frequency modulation of the system. Wind speed data comes from actual data from the San Cristobal Wind Farm. The revised IEEE RTS-79 system diagram is shown in Figure 7.

5.2 Results of IEEE RTS79 system

Figure 8 shows the improvement effect of wind turbines participating in system frequency control on the maximum deviation of system frequency $\Delta f_{\max}$ under different wind speeds. In the wind speed range of 7.2–12 m/s, the wind turbine operates in the maximum power point tracking mode. As the wind speed increases, the frequency improvement effect brought by the wind turbine gradually increases. However, when the wind speed is lower than 7.2 m/s and higher than 12 m/s, the trend of the frequency improvement effect of wind turbines changes. When the wind speed is between 3 m/s ~ 7.2 m/s, the wind turbine operates in startup mode. Since the rotor speed variable range is very small in this mode, the frequency support for the power grid is limited. Similarly, when the wind speed is between 12 and 13.2 m/s, the wind turbine operates in constant speed mode and the output power is close to the rated power, which means that the additional power for frequency control is also limited (Liu et al., 2023). When the wind speed is greater than 13.2 m/s, due to security constraints, the wind turbine operating in constant power mode is limited by the rated power and maximum rotor speed. Then, it cannot increase its active output power. Therefore, the wind turbine cannot provide frequency support in this mode.

TABLE 5 The system reliability evaluation result of the provincial power system.

Index	Situation 1	Situation 2
M_{EENS} (MWh/year)	1.10	1.06
M_{EIENS}	0.37	0.35

This case study demonstrates the feasibility of applying the proposed model to practical power systems. However, it is worth noting that the impacts of system frequency on component reliability parameters are necessary to be considered.

When the natural wind speed is 13.2 m/s, the wind turbines are clustered considering the wake effects. First, the wind speed of wind turbines was studied when the wind direction was 0°, as shown in Figure 9. It can be seen from Figure 9 that the wake effect has a great influence on the wind speed of the wind turbine. Therefore, it is necessary to cluster the wind turbines according to the wind speed and establish an equivalent model of the wind turbine. Table 2 shows the clustering results of wind turbines in four cases where the wind speed direction is 0°, 18°, 32° and 45°.

Figure 10 shows the natural wind speed of the wind turbine cluster is 13.2 m/s, and the wind speed of each wind turbine in different wind directions. The same wind speed is drawn in the same color. Comparing the data in Figure 10 and Table 2, it can be found that the clustering algorithm proposed in this article can cluster wind turbines with similar wind speeds into the same group, and then the equivalent wind turbine cluster model can be used, which greatly improves the efficiency of calculating frequency performance indicators.

Then we illustrate the accuracy of the proposed model by comparing the evaluation results of power system frequency performance-reliability with and without considering the impacts of frequency performance on the system reliability level.

Assuming that the predicted wind speed is 13.2 m/s, and the actual wind speed is 12 m/s. The absolute error of wind speed prediction is 1.2 m/s. Table 3 shows the results of the frequency performance and reliability of the power system. Situation 1 refers to considering the impacts of frequency performance on the reliability parameters of generation units. Situation 2 refers to without consideration of the impacts. From the perspective of frequency indicators, the frequency limit expectation M_{ENUF}, low-frequency duration expectation M_{EUFD}, low-frequency event occurrence probability M_{LFEP} and system recovery probability M_{PRLFE} corresponding to Situation 1 are 102%, 108%, 100%, and 101.25% than the ones related to Situation 2. From the perspective of system reliability indicators, the expected power shortage M_{EENS} and the indirect expected power shortage M_{EIENS} corresponding to Situation 1 are 102% and 103% than the ones related to Situation 2. This shows that when the impacts of frequency performance on the reliability parameters of generation units are not considered, the reliability level of the generation units is overestimated, resulting in overly optimistic frequency performance and power system reliability evaluation results. On the other hand, the expected frequency M_{ENUF} corresponding to Situation 1 reaches 4,867.4 times/year, and the expected low-frequency duration M_{EUFD} reaches 161.7 h/year. This shows that the reliability risks caused by frequency exceeding limits in power systems including wind power cannot be ignored.

The model proposed in this article simultaneously considers two factors: 1) the frequency regulation capability of wind turbine clusters with wake effects, and 2) the dependence of system frequency performance and generator unit reliability parameters. To illustrate the necessity of considering these two factors, four types of situations are set up for comparison:

Situation A: Both 1) and 2) are considered.

Situation B: Consider 1), but do not consider 2); that is, the dependence of the system frequency performance on the reliability parameters of the generator is ignored.

Situation C: Consider 2), but do not consider 1). Namely, the wake effect is not ignored.

Situation D: Neither factor is considered; that is, the traditional power system reliability assessment method.

Existing studies fall into three categories: Situations B to D. Table 4 shows the system's expected power shortage M_{EENS} and indirect expected power shortage M_{EIENS} under four types of situations. Since traditional reliability assessment does not consider the impact of the frequency modulation process, there is no corresponding indirect expected power shortage M_{EIENS}. Scenario A considers more comprehensive factors and can reflect more objective frequency performance and reliability evaluation results. The factors considered in scenarios B and C are lacking, and the corresponding expected power shortage M_{EENS} and indirect expected power shortage M_{EIENS} are smaller than those in scenario A, and the results are too optimistic.

5.3 Results of a provincial power system

To verify the accuracy and scalability of the proposed method, a provincial power system located in China is employed as the testing ground. This system encompasses a considerable scale, comprising 220 generators, 1,393 buses, and 2033 transmission lines. The peak load within this provincial system reaches 38,760 MW, with an installed capacity of 64,471 MW. Notably, the enumeration of branch and generator outages is conducted up to the N-3 contingency level, while branch outages are solely enumerated up to the N-1 contingency level. For evaluation, a period of 6 h is chosen. The reliability evaluation outcomes are presented in Table 5, where Situation 1 refers to considering the impacts of frequency performance on the reliability parameters of generation units and Situation 2 refers to without consideration of the impacts.

6 Conclusion

This paper investigates the dependence between the power system reliability level and the system frequency performance. In this study, a power system frequency regulation model is developed that considers the regulation capabilities of wind turbines. Subsequently, an equivalent wind turbine cluster is integrated into the frequency regulation architecture of thermal power units, thereby facilitating the analysis of frequency performance. The frequency performance of the power system, considering the uncertain operation conditions and random faults of generating units, is then quantitatively examined. A model for the frequency-dependent reliability parameters of generators is derived. Furthermore, a multi-time scale co-evaluation framework is proposed to enable the simultaneous evaluation of frequency performance and operational reliability. The proposed methodology is applied to case studies involving the modified IEEE RTS-79 system and a provincial power system. The results demonstrate that the proposed approach achieves efficient determination of frequency performance and reliability outcomes, surpassing the capabilities of existing research in this domain.

Furthermore, the suggested evaluation method can be integrated into the framework of power system optimal dispatching and planning. Given the imperative coordination of economic considerations, reliability requirements, and frequency stability, it becomes essential to establish an effective long-term capacity planning approach for the power system. This methodology ensures the optimal arrangement of generating units and guarantees the system's sustained capacity adequacy over the long term. By incorporating the proposed evaluation method into the planning process, power system operators can make informed decisions regarding the configuration of generating units, striking a balance between economic efficiency, operational reliability, and the safeguarding of frequency stability.

Data availability statement

The raw data supporting the conclusion of this article will be made available by the authors, without undue reservation.

Author contributions

ML: Funding acquisition, Writing–original draft, Writing–review and editing. YZ: Conceptualization, Formal Analysis, Methodology, Writing–review and editing. LZ: Data curation, Investigation, Software, Supervision, Writing–review and editing. QC: Data curation, Formal Analysis, Project administration, Supervision, Validation, Writing–review and editing. DC: Funding acquisition, Resources, Visualization, Writing–review and editing.

Funding

The author(s) declare financial support was received for the research, authorship, and/or publication of this article. This work was supported by the Key Science and Technology Project of China Southern Power Grid under a grant (No. 066500KK52222013).

Conflict of interest

Authors ML and LZ were employed by Power Dispatching and Control Center of Guizhou Power Grid Company. Author DC was employed by China Southern Power Grid.

The remaining authors declare that the research was conducted in the absence of any commercial or financial relationships that could be construed as a potential conflict of interest.

Publisher's note

References

Attabo Ameh, A., Ajayi Oluseyi, O., Oyedepo Sunday, O., and Afolalu Sunday, A. (2023). Assessment of the wind energy potential and economic viability of selected sites along Nigeria's coastal and offshore locations. *Front. Energy Res.* 11, 1186095. doi:10.3389/fenrg.2023.1186095

Chao, H., Hu, B., Xie, K., Tai, H. M., Yan, J., and Li, Y. (2019). A sequential mcmc model for reliability evaluation of offshore wind farms considering severe weather conditions. *Ieee Access* 7 (1), 132552–132562. doi:10.1109/access.2019.2941009

Chen, L., Wang, P., Han, X., Qin, W., Billinton, R., and Li, W. (2017). Operational reliability and economics of power systems with considering frequency control processes. *Ieee Trans. Power Syst.* 32 (4), 2570–2580. doi:10.1109/tpwrs.2016.2632157

Ding, J. (2022). *Reliability evaluation and tracing for power systems integrated with wind power considering epistemic uncertainty [D]*. Chongqing: Chongqing University.

Ding, Y., Shao, C., Hu, B., Bao, M., Niu, T., Xie, K., et al. (2021). Operational reliability assessment of integrated heat and electricity systems considering the load uncertainties. *Ieee Trans. Smart Grid* 12 (5), 3928–3939. doi:10.1109/tsg.2021.3081602

Farivar, G. G., Manalastas, W., Tafti, H. D., Ceballos, S., Sanchez-Ruiz, A., Lovell, E. C., et al. (2022). Grid-connected energy storage systems: State-of-the-art and emerging technologies. *Proc. IEEE.*

Hu, B., Pan, C., Shao, C., Xie, K., and Niu, T. (2021). Decision-dependent uncertainty modeling in power system operational reliability evaluations. *Ieee Trans. Power Syst.* 36 (6), 5708–5721. doi:10.1109/tpwrs.2021.3081765

Huang, L., Wu, C., Zhou, D., Chen, L., Pagnani, D., and Blaabjerg, F. (2023). Challenges and potential solutions of grid-forming converters applied to wind power generation system—An overview. *Front. Energy Res.* 11, 1040781. doi:10.3389/fenrg.2023.1040781

Kundur, P., and Malik, Om (2022). *Power system stability and control [M]*. 2nd Edition. New York: Mcgraw-Hill Education.

Lei, J., Yuan, Z., Bai, H., Su, S., Yang, J., Li, W., et al. (2022). Economic dispatch of distribution network with dispersed wind power considering network reconfiguration. *Front. Energy Res.* 10 (2022), 942350.

Li, W. (2013). *Reliability assessment of electric power systems using Monte Carlo methods*. Springer Science & Business Media, 2013.

Lin, C., Hu, B., Shao, C., Li, W., and Xie, K. (2022a). Delay-dependent optimal load frequency control for sampling systems with demand response. *IEEE Trans. Power Syst.* 37 (6), 4310–4324. doi:10.1109/tpwrs.2022.3154429

Lin, C., Hu, B., Shao, C., Niu, T., and Cheng, Q. (2022b). An analysis of delay-constrained consensus-based optimal algorithms in virtual power plants. *Isa Trans.* 125, 189–197. doi:10.1016/j.isatra.2021.06.035

Lin, C., Hu, Bo, Shao, C., Ye, Y., Tai, H. M., Xie, K., et al. (2023). Event-triggered load frequency control based on age-of-information. *IEEE Trans. Power Syst.* 38 (3), 2348–2361. doi:10.1109/tpwrs.2022.3186333

Liu, Y., Wang, Y., Wang, Q., Zhang, K., Qiang, W., and Wen, Q. (2023). Recent advances in data-driven prediction for wind power. *Front. Energy Res.* 11, 1204343. doi:10.3389/fenrg.2023.1204343

National development and reform commission of China (2022). *China's renewable energy development in 2022*. Available at: https://www.ndrc.gov.cn/fggz/hjyzy/jnhnx/202302/t20230215_1348799.html.

National Power Grid Operation And Control Standardization Technical Committee (2023). *Guidelines for power system security and stability: gb38755-2019 [M]*. Beijing: China Standard Press.

Owens, C. (2019). *Blackout – everything you need to know [Z]*. Available at: Https://Www.Theblackoutreport.Co.Uk/2021/08/09/9-August-2019-Blackout/(Accessed August 9, 2019).

Shafi, A., Hussein, S., and Shima, H. (2020). Design of optimal power point tracking controller using forecasted photovoltaic power and demand. *Ieee Trans. Sustain. Energy* 11 (3), 1820–1828. doi:10.1109/tste.2019.2941862

Sharifinia, S., Rastegar, M., Mehdi, A., and Fotuhi-Firuzabad, M. (2020). Inverse reliability evaluation in power distribution systems. *Ieee Trans. Power Syst.* 35 (1), 818–820. doi:10.1109/tpwrs.2019.2952518

Tang, Y., Yang, C., Yan, Z., Xue, Y., and He, Y. (2022). Coordinated control of a wind turbine and battery storage system in providing fast-frequency regulation and extending the cycle life of battery. *Front. Energy Res.* 10, 927453. doi:10.3389/fenrg.2022.927453

Wang, Y., Vijay, V., Mojdeh, K., and Singh, C. (2020). Composite system reliability evaluation with essential reliability services assessment of wind power integrated power systems. *Ieee Open Access J. Of Power And Energy* 7 (1), 403–413. doi:10.1109/oajpe.2020.3029119

Wu, T., and Wang, J. (2023). Reliability evaluation for integrated electricity-gas systems considering hydrogen. *Ieee Trans. Sustain. Energy* 14 (2), 920–934. doi:10.1109/tste.2022.3229896

Wu, X., Shen, Z., Fan, X., and Yang, L. (2023). Short-term wind power prediction based on anomalous data cleaning and optimized lstm network. *Front. Energy Res.* 11, 1268494. doi:10.3389/fenrg.2023.1268494

Yang, X., Yang, Y., Liu, Y., and Deng, Z. (2020). A reliability assessment approach for electric power systems considering wind power uncertainty. *Ieee Access* 8 (1), 12467–12478. doi:10.1109/access.2020.2966275

Ye, C., Guo, L., Ding, Y., Ding, M., Wang, P., and Wang, L. (2023). Reliability assessment of interconnected power systems with hvdc links considering frequency regulation process. *J. Of Mod. Power Syst. And Clean Energy* 11 (2), 662–673. doi:10.35833/mpce.2021.000491

Zhang, T., Yan, X., Zhang, R., Ye, Q., and Ma, J. (2022). Optimized dispatching for integrated energy system with wind power. *Front. Energy Res.* 10, 917805. doi:10.3389/fenrg.2022.917805

Zhao, X., Lin, Z., Fu, B., and Gong, S. (2021). Research on frequency control method for micro-grid with a hybrid approach of FFR-OPPT and pitch angle of wind turbine. *Int. J. Of Electr. Power and Energy Syst.* 127 (1), 106670. doi:10.1016/j.ijepes.2020.106670

Zhou, Z., Shi, L., and Chen, Y. (2021). An optimal over-frequency generator tripping strategy for regional power grid with high penetration level of renewable energy. *J. Mod. Power Syst. Clean Energy* 9 (5), 1007–1017. doi:10.35833/MPCE.2020.000374